Journal of Scientific & Industrial Research
Vol. 68, September 2009, pp. 775-782

Three dimensional simulation of fatigue crack growth in friction stir welded joints of 2024-t351 Al alloy

M Zadeh, Aidy Ali, A F Golestaneh and B B Sahari

Department of Mechanical and Manufacturing Engineering, Faculty of Engineering, University Putra Malaysia, 43400 Serdang, Selangor, Malaysia

Received 15 January 2009; revised 18. May 2009; accepted 26 May 2009

Present paper predicts fatigue life and crack growth behaviour of Al 2024-T351 friction stir welded joint by boundary element method, using professional software package FRANC3D. Crack propagation is analyzed for residual stress and stress relaxation in different friction stir welding (FSW) regimes under cyclic loads. Linear elastic fracture mechanics model is applied and simulated parameters are verified with analytical and experimental observations.

Keywords: Fatigue crack growth; Friction stir welding; FRANC3D

Introduction

Friction stir welding (FSW), widely used for joining Aluminium (Al) alloys in aircraft components, is suspected to include minor cracks leading to fatigue crack propagation phenomenon in the joint. Fatigue crack growth process is categorized into stages: i) initiation and early crack growth ii) stable crack growth; and iii) fracture instability. Paris *et al*[1] introduced a simple engineering model based on empirical observations. Hobson-Brown model[2] governs first and second crack growth stages. Navaro Rios model[3] is capable of fatigue crack growth prediction in all three propagation steps. Forman-Newman-de Koning model[4,5] is considering retardation phenomenon near threshold, acceleration near fracture and incorporate load ratio (R) as an effective parameter in analysis.

As FSW method is mostly used for joining Al alloys, Booth *et al*[6] and Ali *et al*[7] characterized fatigue behaviour of FSW joint of Al 2024-T351. Dalle Donne *et al*[8] also worked on FSW Al 2024-T3 joints metallographically and analyzed hardness of its regions. Other series of Al alloys are also characterized in terms of fatigue parameters[9-16]. Bussu & Irving[17] showed that crack growth behaviour in FSW joints is generally dominated by weld residual stress in comparison with microstructural and hardness characteristics of FSW regimes. Borino *et al*[18] worked on failure in FSW joints using experiments and Finite Element Analysis (FEA). Ghindi *et al*[19] simulated fatigue crack propagation of FSW joints under flight loading conditions and validated by experiments. Fracture mechanics parameters of each of FSW joint regimes are different from each other[20].

In order to analyze crack growth in an integrated system of analysis, present model has been developed to simulate crack in FSW joint in three dimensions by boundary element method using FRANC3D a fracture mechanics software package.

*Author for correspondence
Tel: +6 017 202 0544; Fax: +6 038 656 7122
E-mail: zadeh_mohammadim2@asme.org

Proposed Model

Modelling and Simulation

Numerical Analysis

Stress intensity factor (SIF) is used as fracture criterion, in order to simulate fatigue crack growth behaviour of FSW joint using boundary element method. SIF should be calculated near crack tip area. SIFs are computed using displacement correlation technique in first row of mesh nodes behind crack front or points located at the area of constant distance from crack front. FSW method is used in order to join two rectangular plates of Al 2024-T351 in specific dimensions and it is tested under four point bending fatigue test. In this study, four main regimes have been modelled (Fig. 1). OSM (Object Solid Modeller), a simple object oriented geometric modeller, was used to generate geometric descriptions of elements suitable for importing into FRANC3D.

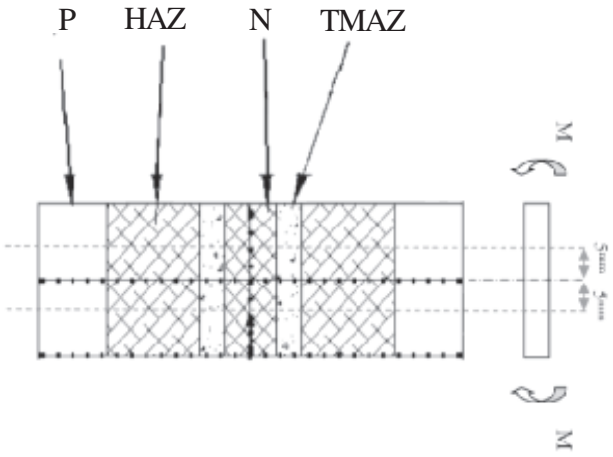

Fig. 1—Simulation using symmetric characteristics of specimen

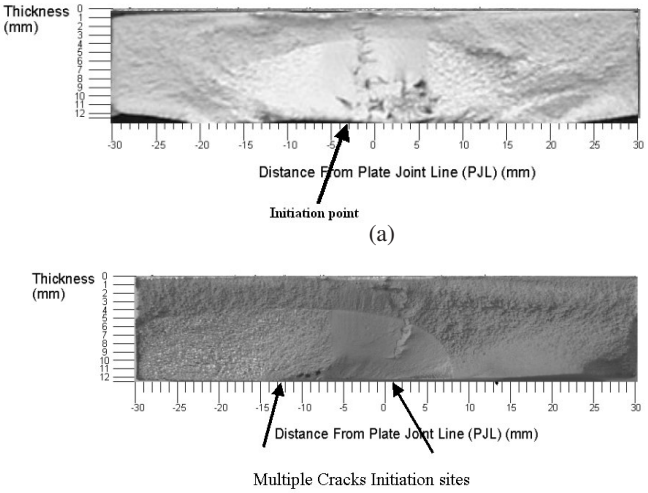

Fig. 2—Replication images for HCF of 2024-T351 Al Alloy FSW specimen: a) Polished mirror FSW joint under 270 MPa maximum applied stress with load ratio R= 0.1; and b) As welded FSW joint under 161 MPa maximum applied stress with load ratio R= 0.1

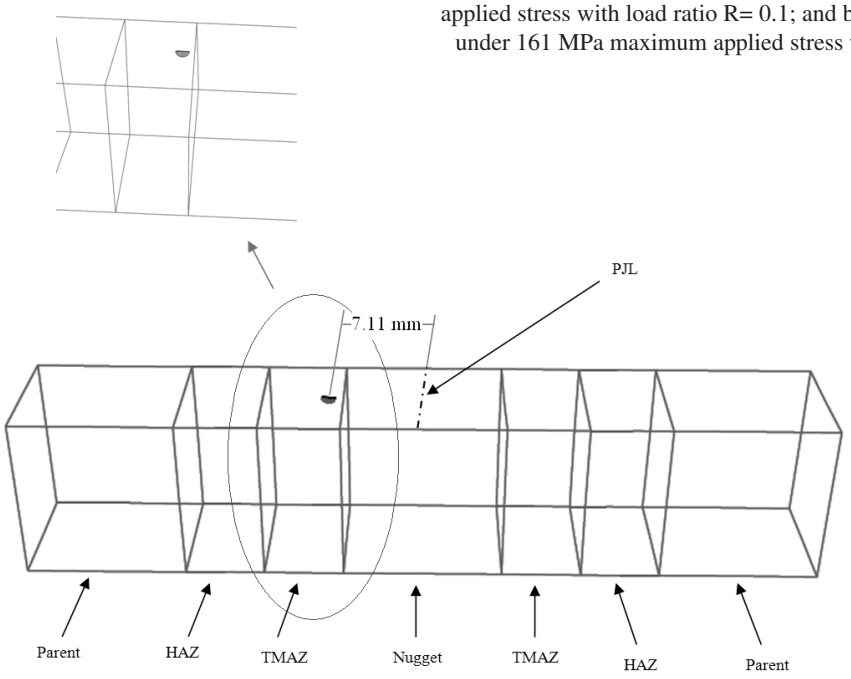

Fig. 3—Schematic image of initial crack location in developed model

In experiments, smallest individual surface crack lengths in a FSW joint detected from replication were 0.62 mm long for 300 MPa and 0.112 mm long for 270 MPa maximum applied stresses[20]. As maximum stress values applied in present work are mostly above 300 MPa (Low cycle fatigue regime), a 1 mm long crack is introduced in TMAZ region, which is weakest regime with lowest strength among other FSW regimes. A semi-circular shape was chosen to represent initial crack observed during experiment[20]. Relationship between crack length and depth in semi-circular crack has been defined[17] as

Half crack length / crack depth = 1.02-1.07 …(1)

Mid value (1.05) is considered and crack depth is calculated as 0.47 mm. According to replication (Fig. 2), initiation site of 2024 Al alloy FSW under maximum stress of 270 MPa and 161 MPa with load ratio R=0.1 are about 5 mm and 12 mm far from plate

Table 1-Mechanical and fracture mechanics characteristics of specimen15

Regimes	Fracture toughness Mpa√m	Modulus of elasticity MPa	Yield strength MPa	Poisson ratio
Nugget	30.3	68 x 10^3	350	0.33
TMAZ	23.5	68 x 10^3	272	0.33
HAZ	38.7	68 x 10^3	448	0.33
Parent	32.0	68 x 10^3	370	0.33

joint line (PJL) respectively for high cycle fatigue (HCF) testing. First figure (Fig. 2a) is for polished mirror FSW specimen, while other one is for welded FSW specimen; therefore, two initiation sites (Fig. 2b) under lower value of stress can be observed. In present simulation, as maximum applied stress is considered 318.7 MPa after incorporating stress relaxation phenomenon, crack was initiated 7.1 mm far from PJL in TMAZ (Fig. 3).

In present model, four sets of material properties were assigned to four different regimes (Table 1). Bending moment was applied using constant traction and compressive stress distributions along models' edges. At this stage, a specific stress distribution[20] was introduced and stress range ($\Delta\sigma = 243$ Mpa) with load ratio (R= 0.1) was applied to the model. Residual stress (σ_{res}) in a FSW joint varies through depth (Fig. 4). Tensile residual stress (max. 96 Mpa) is used in this simulation analysis as

$$\sigma_{Max-applied} = \sigma_{Max} + \sigma_{res} \quad \ldots(2)$$

For applied stress range $\Delta\sigma$, 243 MPa and R, 0.1, maximum applied stress ($\sigma_{Max-applied}$) becomes 366 MPa. According to constitutive properties of model (Table 1), calculated applied value (272 Mpa) exceeds yield strength of material in TMAZ and residual stress relaxation phenomenon should be considered according to Ramberg-Osgood equation as

$$\frac{366}{E} = \frac{\sigma}{E} + \left(\frac{\sigma}{800}\right)^{\frac{1}{0.1266}} \quad \ldots(3)$$

Therefore, $\sigma_{Max-applied}$ after relaxation is 318.7 MPa for modulus of elasticity (E) at 68 GPa.

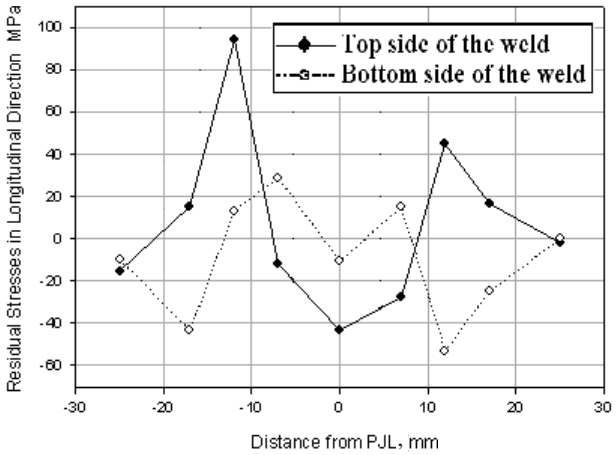

Fig. 4—Longitudinal residual stress distribution along FSW 2024-T351 Al alloy joint20

Discretization and meshing process were done using edge discretization approach. A quadrilateral 20 node element was used to mesh entire model except area near crack, which has been meshed using triangular elements to provide finer mesh. Triangular elements get finer after each step of crack propagation during every remeshing process (Fig. 5). Crack propagation process is based on SIF values, which were calculated using displacement correlation method. To find propagation direction, in each step, 2D plane strain equations were evaluated at discrete points along crack front. Growth increments were calculated using Paris equation. Four different fracture mechanics characteristics of FSW joint make propagation process more complicated as crack approaches new material properties during propagation process. This affects on further SIF calculations and in some cases it can lead to considerable errors in SIF values near crack tip approaching new material boundary. Propagating crack in each regime and storing results as a propagation history help to overcome probability of encountering such errors during simulation. Combining these history data can lead to achieve total life estimation of cracked model under specified stress distribution and loading condition. In three-dimensional simulation of crack propagation in this study, effect of deviation of crack propagation from original crack plane is also considered in final numerical solution. Fig. 6 shows how crack tips start to deviate from original crack plane after 10 steps of propagation under maximum stress (300 Mpa). Fracture mechanics models (Paris and Forman-Newman-de Koning models) are used in computational model. Paris model is used for simplicity and accurate results in LEFM region of crack propagation as simulation is based on SIF calculation with least error.

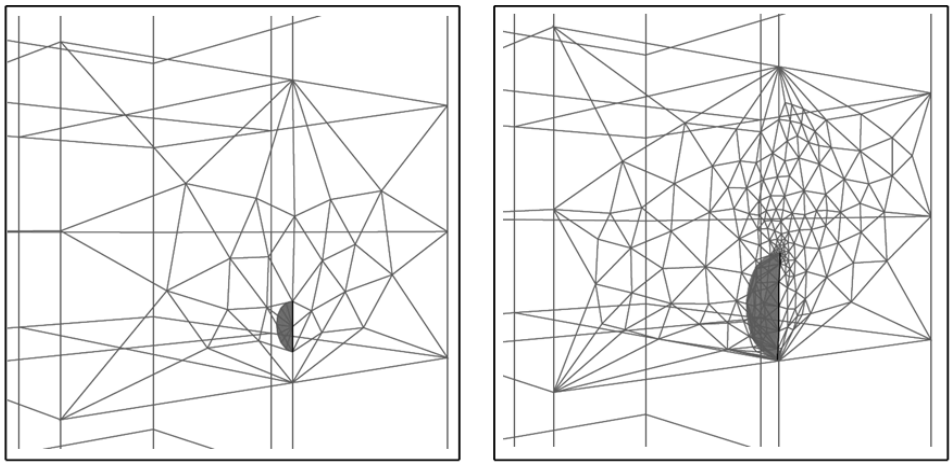

Fig. 5—Meshing distribution around crack tip: a) First step after initiation; and b) Remeshed area after 4 steps of propagation

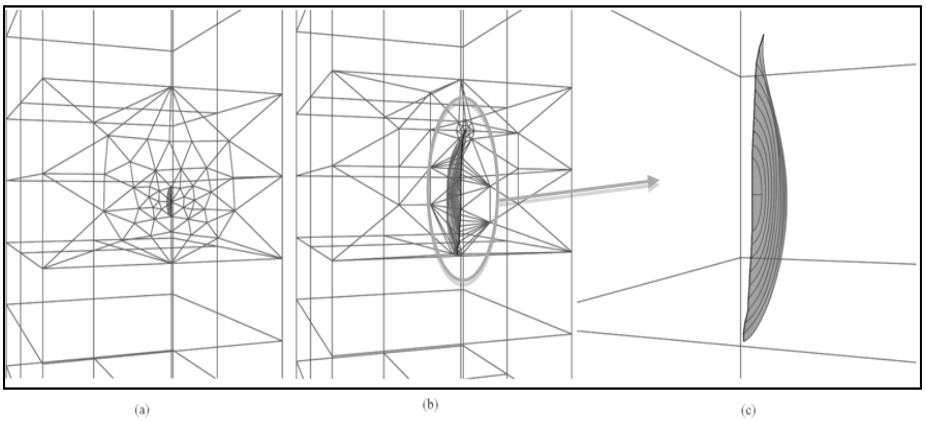

Fig. 6—Crack growth profile under σ=300 Mpa: a) Initiation of 1 mm crack in specimen; b) Crack profile after 10 steps of propagation; and c) Crack starts to deviate from its original plane after 10 steps of propagation

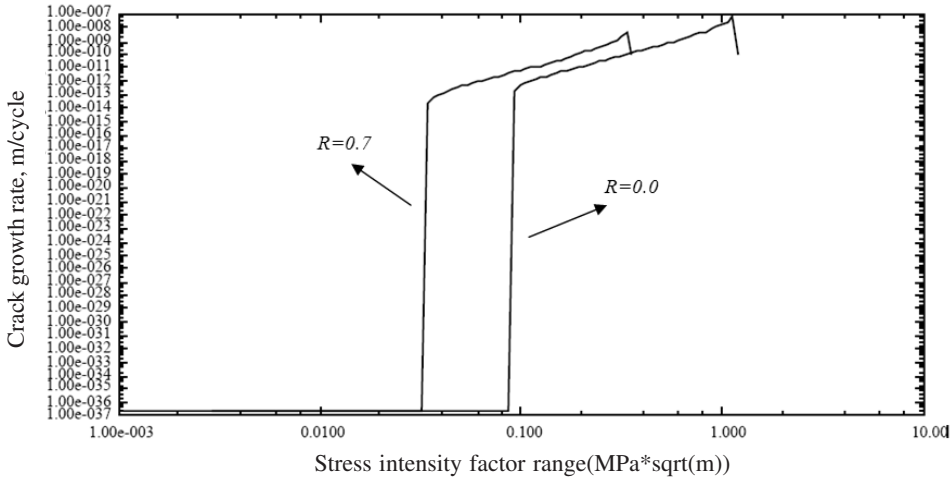

Fig. 7—Crack growth rate data for Al 2024-T351 with different load ratios

Table 2—Paris constants for Al 2024 T351[12]

FSW Regimes	m	C (cycle)$^{-1}$
Parent	2.400	2.035 ´ 10^{-10}
Nugget	3.106	2.023 ´ 10^{-10}
TMAZ	2.254	3.987 ´ 10^{-10}
HAZ	2.280	8.410 ´ 10^{-11}

Table 3—Comparison between numerical and analytical solutions

Crack length mm	Numerical cycles	Analytical cycles	Error %
1.00	2.0750e6	2.07500e6	0.0000
1.75	2.0865e6	2.07833e6	0.0039
2.00	2.0890e6	2.08167e6	0.0035
2.40	2.0923e6	2.08667e6	0.0027
3.90	2.1023e6	2.13167e6	-0.0138
4.30	2.1072e6	2.13711e6	-0.0140
7.10	2.1590e6	2.20000e6	-0.0186

$$\frac{da}{dN} = C(\Delta K)^m \qquad \ldots(4)$$

where *a,* half length of surface crack; *N*, number of cycles; ΔK, SIF range; *C* & *m,* Paris constants.

Fracture mechanics analysis has been done for each FSW regime separately based on SIF calculations. Paris constants for Al 2024-T351 are reported[17] (Table 2). As Paris model governs only second region of propagation process, which almost comply with linear behaviour, Forman-Newman-de Koning model is used to simulate first and third crack growth regions more accurately as

$$\frac{da}{dN} = \frac{C(1-f)^n \Delta K^n \left[1-\frac{\Delta K_{th}}{\Delta K}\right]^p}{(1-R)^n \left[1-\frac{\Delta K}{(1-R)K_c}\right]^q} \qquad \ldots(5)$$

where, *C*, *n*, *p* and *q* are empirical constants derived through curve fitting of test data; ΔK_{th} is threshold stress intensity factor range and *f* is a function to incorporate effect of *R* for plasticity induced crack closure under constant amplitude loading[4] as

$$f = \begin{cases} Max\ (R, A_0 + A_1 R + A_2 R^2 + A_3 R^3) \\ A_0 + A_1 R \end{cases} \qquad \ldots(6)$$

$$A_0 = (0.825 - 0.34\alpha + 0.05\alpha^2)\left[\cos\left(\frac{\pi}{2} S_{max}/\sigma_0\right)\right]^{1/\alpha} \qquad \ldots(7)$$

where, $A_1 = (0.415 - 0.071\alpha) S_{max}/\sigma_0$,

$A_2 = 1 - A_0 - A_1 - A_3$, $A_3 = 2A_0 + A_1 - 1$

Plane stress / strain constraint factor as α and ratio between maximum applied stress to material flow stress is depicted as S_{max}/σ_0. Both are treated as fitting parameters in this model[4]. Constants and fracture mechanics parameters needed for this model are obtained from NASGRO database for Al 2024-T351 as follows: Ultimate tensile stress UTS, 468.8 MPa; uniaxial yield stress YS, 372.3 MPa; part through toughness K_1, 1667.9 MPa√m; planes stress toughness K_2, 1181.4 MPa √m; plane stress/strain parameter A_k, 1; plane stress/strain parameter B_k, 1; FNK crack growth constant *C*, 1.6×10^{-12} ; FNK crack growth exponent *n*, 3.353; FNK crack growth exponent *p*, 0.5; FNK crack growth exponent *q*, 1; Threshold stress intensity factor range (at *R*=0) ΔK_{th}, 90.3 MPa√m; α, 1.5; and S_{max}/σ_0, 0.3. Crack growth rate of Al alloy is illustrated (Fig. 7) for different load ratio values.

Analytical Model

An analytical model characterizes fatigue behaviour of a FSW joint of Al 2024-T351. Although numerical methods predict fatigue behaviour of welding joint with a good compliance with experiments, analytical model can provide a knowledgeable insight of whole problem especially when numerical process includes some assumptions for simplification. Hobson-Brown model[2] is adopted for analytical study. In order to evaluate results from numerical analysis, results were compared with analytical work (Table 3). Statistical analysis on evaluation of errors in each step of crack propagation (Table 3) is shown in order to observe accuracy of numerical model in comparison. Simulated model showed good agreement with analysis. Comparison between analytical and experimental results has also been studied[20].

Simulation and analytical results show good agreement (Fig. 8). Results from Forman-Newman-de Koning model get closer to analytical results rather than

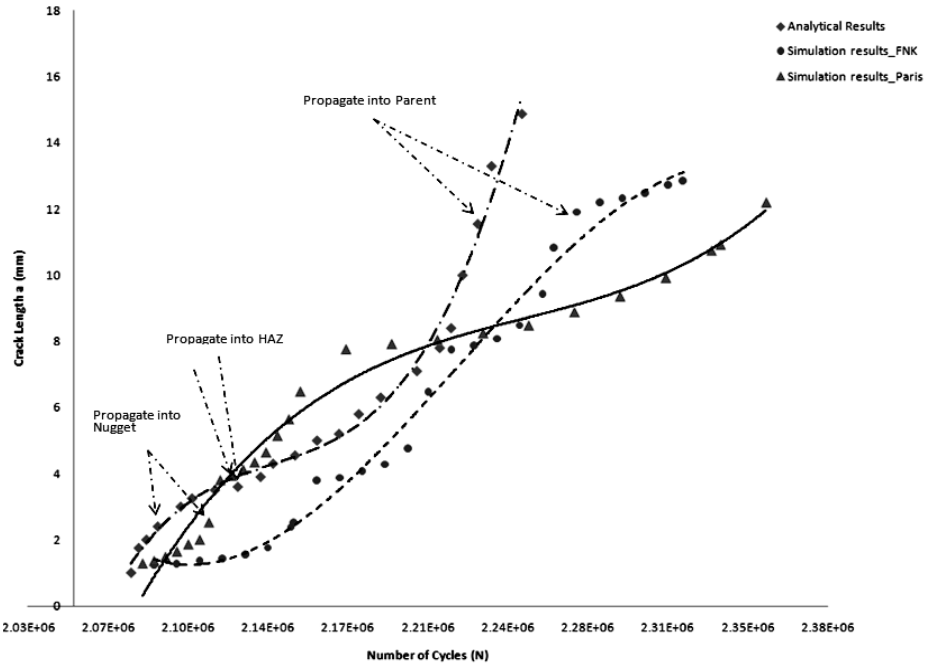

Fig. 8—Total crack length versus number of cycles for 270 MPa maximum applied stress with load ratio R= 0.1

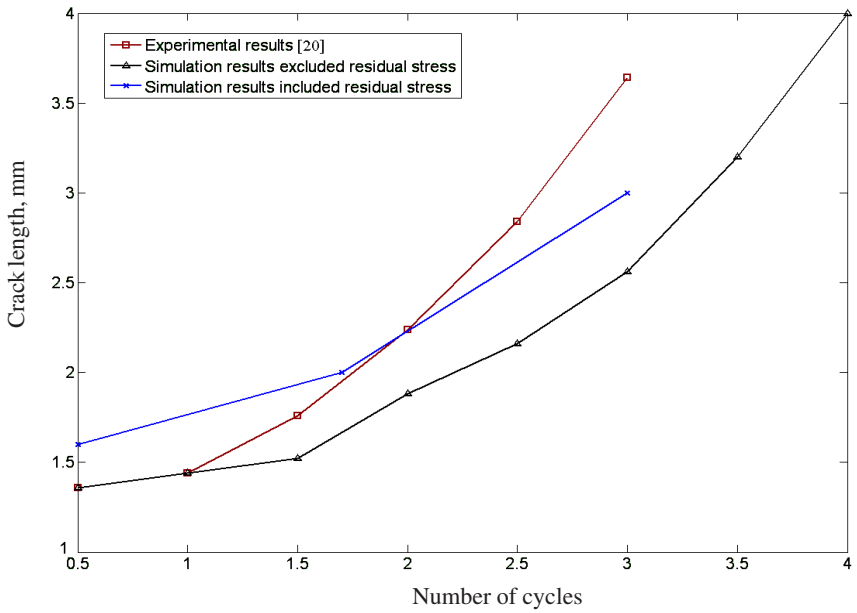

Fig. 9—Effect of residual stress on simulation result in comparison with experiment (Crack propagation under max. stress of 270 MPa and R= 0.1)

results from Paris model, because Paris model provides good predictions during second region of crack propagation process. Forman-Newman-de Koning can predict crack propagation behaviour well especially near fracture point where propagation process accelerates from its rate in second region. Therefore, Forman-Newman-de Koning model shows better compliance (Fig. 8). As it was expected, most number of cycles is predicted precisely using Paris model applied in numerical analysis and Forman-Newman-de Koning model shows better agreement in results near fracture. Deviation of numerical results from analytical ones in farthest points is less than 10%, which is an acceptable range for such a simulation.

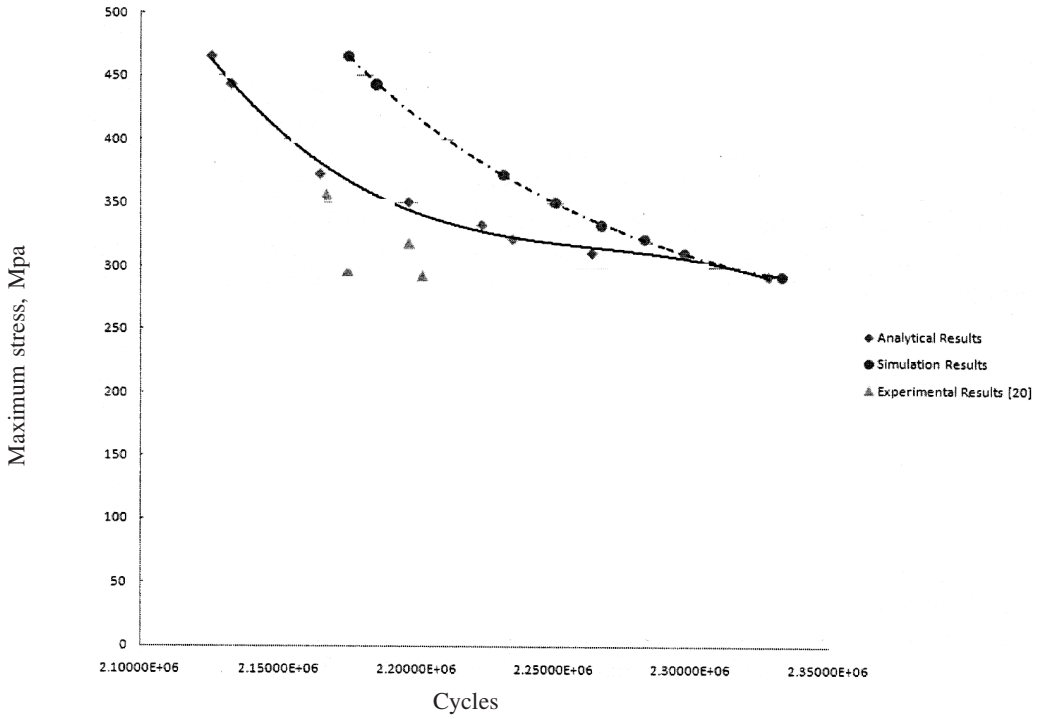

Fig. 10—Life prediction of Al 2024-T531 FSW joint

Results and Discussion

Effect of Residual Stress

In order to observe importance of residual stress, stress distribution pattern with stress range ($\Delta\sigma = 243$ Mpa) is considered without incorporating residual stress. Results obtained from this situation as compared with other results (Fig. 9) indicated that incorporating residual stress into numerical analysis leads to more accurate results comparing with real situation.

Fatigue Life Prediction

In order to perform life estimation process based on fatigue phenomenon, 13 different stress distribution patterns through different stress ranges were applied in developed model through separate simulation processes. Each FSW regime is considered under these stress distribution conditions and crack growth history in each regime has been recorded. With accumulation of all simulated results, lifespan of FSW joint is obtained (Fig. 10), showing good compliance between simulation and analytical results especially in lower stress values, however maximum deviation between analytical and simulation results are of 10%. In this graph, Paris model is used in numerical process as it covers more cycles of propagation with good agreement with analytical model. Therefore, as soon as maximum applied stress increases, process of reaching fracture point gets faster. It is expected that Paris shows more deviation as maximum applied stress increases. However, total accordance with highest error of 10% is reasonable. Deviation of experimental results from reported[20] with analytical and numerical results can be from some metallurgical parameters, which affect propagation process through experiments while they are not considered in analytical modelling or in numerical analysis. Parameters like strengthening precipitates occur dominantly in HAZ region of FSW. This phenomenon affects on hardness distribution of the region, which can play a role in microstructural fracture mechanics of the weld.

Conclusions

Crack propagation and life span of FSW joint was studied by fracture mechanics approach using boundary element method and using a professional fracture mechanics software package FRANC3D. Good agreement was observed between computational and analytical models. Paris model was accurate in second region of crack propagation while Forman Newman de-Koning model was accurate in first and third of crack propagation. Results verified with experiments and

analytical method show 90% accuracy in terms of fracture mechanics and fatigue life prediction. Further research can be carried out by incorporating plasticity-induced crack closure and crack blunting phenomena in numerical modelling, in order to being numerical analysis more closer to experimental results.

Acknowledgement

Authors thank University Putra Malaysia (UPM) for financial support and award of fellowship for two authors (M Zadeh and A F Golestaneh).

References

1 Paris P & Erdogan F, A critical analysis of crack propagation laws, *Trans ASME Ser D, J Basic Eng,* **85** (1963) 528-534.

2 Hobson P D, Brown M W & De Los Rios E R, Two phases of short crack growth in a medium carbon steel, in *The Behaviour of Short Fatigue Cracks*, edited by *K J Miller & E R delos Rios* (Mechanical Engineering. Publihers, London) 1986, 441-459.

3 Jata K V, Friction stir welding of high strength aluminium alloys, *Mater Sci Forum*, **331-337** (2000) 1701-1712.

4 Newman J C, A crack opening stress equation for fatigue crack growth*, Int J Fract*, **24** (1984) 131-135.

5 Forman R G & Mettu S R, Behavior of surface and corner cracks subjected to tensile and bending loads in a Ti–6Al–4V alloy, in *Fracture Mechanics: Twenty-Second Symposium ASTM STP 1131* **vol. I**, edited by H A Ernst, A Saxena & D L McDowell (American Society for Testing and Materials, Philadelphia) 1992, 519-546.

6 Booth D & Sinclair I, Fatigue of friction stir welded 2024-T351 aluminium alloy, *Mater Sci Forum*, **396-402** (2002) 1671-1676.

7 Ali A, An X, Rodopoulos C A, Brown M W, O'Hara P, Levers A & Gardiner S, The effect of controlled shot peening on the fatigue behaviour of 2024-T3 aluminium friction stir welds, *Int J Fatigue*, **29** (2007) 1531-1545.

8 Dalle D C & Biallas G, Fatigue and fracture performance of friction stir welded 2024-T3 joints, in *European Conf on Spacecraft Structures, Materials and Mechanical Testing*, Braunschweig, Germany, November 1998.

9 Flores O V, Kennedy C, Murr L E, Brown D, Pappu S, Nowak B M & McClure J C, Microstructural issues in friction stir welded aluminum alloy, *Scr Mater*, **38** (1998) 703-708.

10 Heinz B, Skrotzki B & Eggeler G, Microstructural and mechanical characterization of a friction stir welded Al-alloy, *Mater Sci Forum*, **331-337** (2000) 1757-1762.

11 Jata K V, Sankaran K K & Ruschau J J, Friction stir welding effects on microstructure and fatigue of aluminum alloy 7075-T7451, *Metall Mater Trans A*, **31** (2000) 2181-2192.

12 Kwan Y J, Satio N & Shingematsu I, Friction stir process as a new manufacturing technique of ultrafine grained aluminum alloy, *J Mater Sci Lett*, **21** (2002) 1473-1476.

13 Mahoney M W, Rhodes C G, Flintoff J G, Spurling R A & Bingel W H, Properties of friction stir welded 7075 T651 aluminium, *Metall Mater Trans A*, **29** (1998) 1955-1964.

14 Murr L E, Li Y, Trillo E A, Flores R D & McClure J C, Microstructure in friction stir welded metals, *J Mater Process Manuf Sci*, **7** (1998) 145-161.

15 Sato Y S & Kokawa H, Distribution of tensile property and microstructure in friction stir weld of 6063 Aluminium, *Metall Mater Trans A*, **32** (2001) 3023-3031.

16 Sato Y S, Park S H C & Kokawa H, Microstructure factors governing hardness in friction stir welds of solid solution hardened Al alloys, *Metall Mater Trans A*, **32** (2001) 3033-3042.

17 Bussu G & Irving P E, The role of residual stress and heat affected zone properties on fatigue crack propagation in friction stir welded 2024-T351 aluminum joints, *Int J Fatigue*, **25** (2003) 77-88.

18 Borino G, Fratini L & Parrinello F, Mode I failure modeling of friction stir welding joints, *Int J Adv Manuf Technol*, **41** (2009) 498-503.

19 Ghidini T, Bremen, Polese C, Lanciotti A & Dalle Donne C, Simulations of fatigue crack propagation in friction stir welds under flight loading conditions, *Mater Testing*, **48** (2006) 370-375.

20 Ali A, Brown M W & Rodopoulos C A, Modelling of crack coalescence in 2024-T351 Al alloy friction stir welded joints, *Int J Fatigue*, **30** (2008) 2030-2043.